Sigma J Eng & Nat Sci 35 (1), 2017, 1-22

Sigma Journal of Engineering and Natural Sciences
Sigma Mühendislik ve Fen Bilimleri Dergisi

Research Article / Araştırma Makalesi

A REVIEW: EFFECT OF PRESSURE ON HOMOGENIZATION

Ah Pis YONG[1], Md Aminul ISLAM[1], Nurul HASAN*[2]

[1]*Physical and Geological Sciences Programme, Faculty of Science, Universiti Brunei Darussalam, Jalan Tungku Link, Gadong BE1410, Negara Brunei Darussalam.*
[2]*Petroleum and Chemical Engineering Programme Area, Universiti Teknologi Brunei, Tungku Highway, Gadong BE1410, Negara Brunei Darussalam*

Received/Geliş: 22.05.2016 Revised/Düzeltme: 18.07.2016 Accepted/Kabul: 09.08.2016

ABSTRACT

This review discusses the studies on fluid dynamics passing through in a high-pressure homogenizer in a narrow gap. In industries, such as fine chemical, biotechnology, food and dairy industry, high-pressure homogenization is used to create a stable emulsion in sub-micron or nano drop size. During the homogenization process, high energy input with extreme shear force have to be applied to reduce the droplet sizes for rough or loosely texture emulsion from the smaller scale to a range of nano scale. This process will then can overcome the Laplace pressure. Laplace pressure is the difference in pressure in between the outside and inside of a curving surface. This pressure (100–500 MPa) will then be converted to dynamic energy, therefore prompting a separation of the coarse emulsion into a smaller droplet. Fluid dynamics involved through the homogenising valve is very complicated. In the homogenizer valve, flow conditions expose to intense changes of energy as the fluid goes to low pressure and high speed from high pressure and low speed. To understand these changes, a computational fluid dynamics (CFD) approach is needed. The objectives of this review are the investigation of a dynamic model for describing the dynamics of drop size distributions and the flow pattern in a high-pressure homogenizer. The effect of drop coalescence in droplets is not included because it relies upon the relative rates of drop collision and surfactant adsorption.
Keywords: High-pressure homogenizer, computational fluid dynamics, turbulence.

1. INTRODUCTION

Emulsions are homogeneous mixtures is usually two immiscible phases [1]. Currently, there are several emulsification systems (Table 1). High-pressure homogenization (HPH) is utilised as a part of different modern segments, for example, compound, pharmaceutical, nourishment applications and biotechnology, keeping in mind the end goal is to make emulsions with little drops and limited size distributions with high efficiency [2-4]. Emulsions are thermodynamically shaky, and various procedures hint to changes in the drop size-circulation and emulsion structure [5]. Typically a two-step process is needed for emulsions preparation. To prepare the coarse emulsion (premix), a low shear gadget is utilised. HPH is where the premix will be passed through where the drops are further separated into much littler drops [6-8]. The surface action of

* Corresponding Author/Sorumlu Yazar: e-mail/e-ileti: nurulhasan@asme.org, tel: +6738377501

the emulsifying particles is also expected to be increased with the use of HPH where it might enhance the effectiveness of the item covering capacity or infiltration activity for instance [9]. One of the important characteristics of an emulsion is its distribution of the droplet sizes [10], and, HPH is usually used as a part of experimental examination due to its geometry of the valve which can impacts the droplet disturbance [11]. A stable sub-micron emulsions or nano-emulsion in low-viscosity fluids also can be created by using HPHs [12-15]. Two important factors of the drops, size and distribution magnitude, are considered for stability, reactivity and mouth-feel. In various outlets of the processing industry, it is needed to decrease the size of the droplets and size of the droplets distribution in an emulsion. Through a restricted zone (order 10–100 μm), the emulsion is constrained into by applying a substantial pressure slope (10–100 MPa) [2, 12]

A HPH comprises of a high-pressure cylinder pump and a gap which is narrow. The pressure piston pump usually creates a pressure of 10–500 MPa. A tight gap in the HPH is where the emulsion will be forced to pass through and quickened behind to speed of numerous several m/s. Someplace in the valve restricted area is where the emulsion drops will be break up into small sizes [12, 16]. However, HPH up to 350 MPa has recently gotten awesome consideration. Recently it represents to an imperative advancement since it can be utilised to sterilise items locally [2]. Also, HPH also can be used to adjust the quality of mixtures or a polymeric substance occurring in living organisms, for sustenance or a compound manufactured for use as a medicinal drug [2].

In HPH, a pre-emulsion is accelerated into and forced through a narrow gap and creates a highly turbulent field as the liquid exits the gap into the outlet chamber [17] (Figure 2). In a HPH, the mixture is exposed to intense shear flow fields and turbulent by the change of the pressure to kinetic energy, consequently prompts a separation of the scattered stage into little droplets [9, 18].

Cavitation occurred in the homogenization valve near the entrance and exit of the gap, additionally in the gap itself, great pressure losses occur [13]. In a short distance with a very high speed, as the fluid accelerates, in the middle of the inlet and outlet of the valve, strong pressure gradients occurred, and this creates extreme shear powers and extensional anxiety through the gap in the valve [19].

Figure 1 shows the flow configuration through the homogenising valve. In the valve design of the Stansted Fluid Power Ltd, the high pressure causes the fluid streams through the mobile part of the valve which leads to flow the fluid through the restricted gap with high speed which is framed in between the piston and valve seat. The measurement of the slit (h) and the subsequent stream velocity and pressure of the liquid in front of the valve will rely on upon the major power following up on the valve piston chamber. To manage the homogenising intensity, this can be modified. Homogenising pressure (P_h) is known as the pressure drop of the fluid in the valve.

An extraordinary change is expected at the state of the stream when the fluid goes to low pressure and high speed from high pressure and low speed. The modelling results give complete information on the mechanical stresses and the high shear rates in small disruption valves, and also conceal other phenomena that could not be determined experimentally. The CFD method gives off an impression of being an extremely advantageous way to deal with comprehending these progressions [2, 21, 22].

Table 1. Correlation of various sorts of emulsification framework [20].

Emulsification structure	**Rotor-stator systems**	**High-pressure systems**	**Ultrasonic systems**
Examples	Mixer, agitators, colloid mills (Silverson, Ultra Turrax)	Radial diffusers, valve homogenizers, jet dispersers, microfluidizer	Sonotrodes (sonication probes)
Droplet disruption mechanisms	Shear stress in laminar flow and shear and inertial stress in turbulent flow	Shear and inertial stress in turbulent flow; cavitation in laminar extension flow	Cavitation in micro-turbulent flows
Throughput	Medium to high	High	low
Batch/Continuous	Batch (mixers) or continuous (colloid mills)	continuous	Batch or quasi-continuous
Minimum droplet size (µm)	1.0	0.1	0.1-0.2
Optimal range of viscosity	Low to high	Small to average	Low to medium
Application	Lab/industrial	Lab/industrial	lab
Energy density	Low-high	Medium-high	Medium- high
Change of energy input through	Rotation speed, exposure time, gap distance, and disk design	Pressure, recirculation (exposure time), and nozzle design	Intensity and frequency of ultrasonic wave sonication time
Residence time in dispersing zone, *t*	$0.1 < t < 1$ s	$0.1 < t < 3$ ms	-
Required adsorption rate of emulsifier	Low to high	High to very high	Middle to high

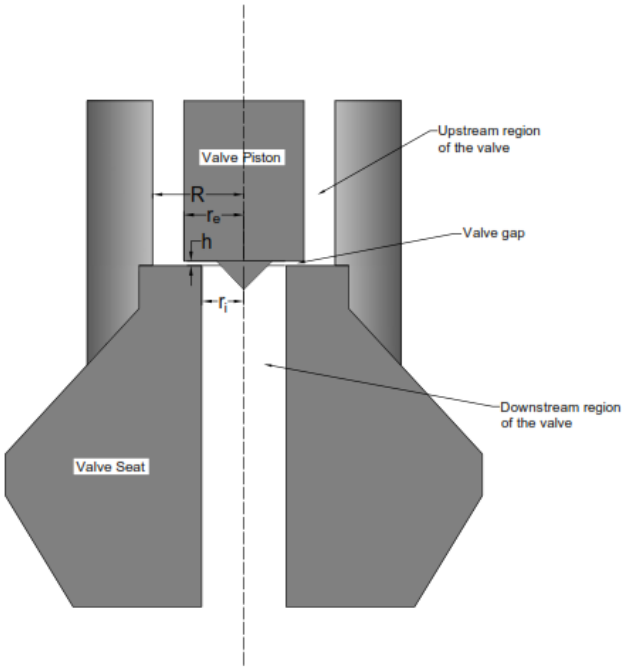

Figure 1. A side view of the Stansted high-pressure homogenising valve [2].

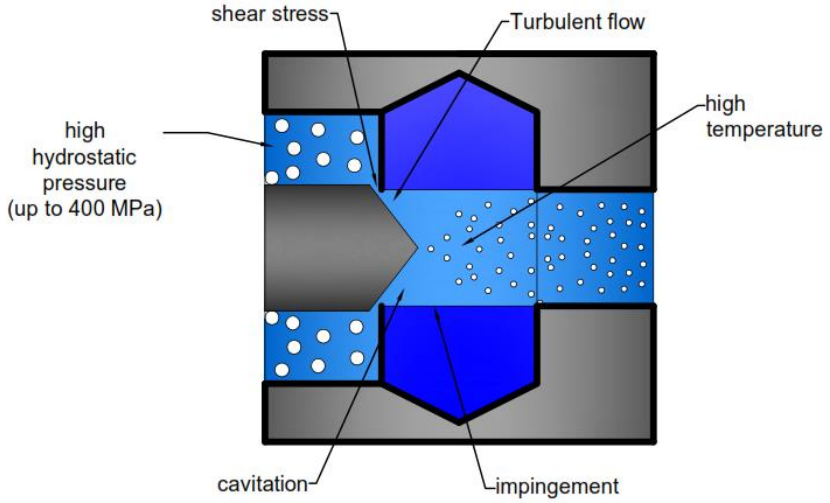

Figure 2. Various physical phenomena are simultaneously affecting a fluid during high-pressure homogenization.

Fragmentation is the process of homogenization as it decreases the drop size to create the fine emulsions and usually to be brought on by cavitation and turbulence. Håkansson, et al. [23] investigated both forms keeping in mind the end goal to discover its area in the HPH valve

region. In the first half of the gap, the tests showed cavitation being concentrated whereas inside the hole, the intensities of the turbulence are very low. At downstream of the narrow gap in the outlet chamber, the turbulence is most effective [24, 25].

Fundamentally downstream of the exit gap, break up occur (Innings and Tragardh, 2005). In HPH the molecule separation begins by a mix of turbulence and laminar shear stress [25, 26].

Kolmogorov–Hinze model has defined the turbulent drop fragmentation. There are two different mechanisms: turbulent inertial (TI) and turbulent viscous (TV) fragmentation (Figure 3). In TI drops are divided by pressure fluctuations actuated by small whirlpools while in TV components by shearing of bigger swirls [23, 27, 28].

Turbulence is said to be the major mechanism compare between laminar shear and cavitation where it prompts the separation of the scattered stage into small droplets [9, 29, 30]

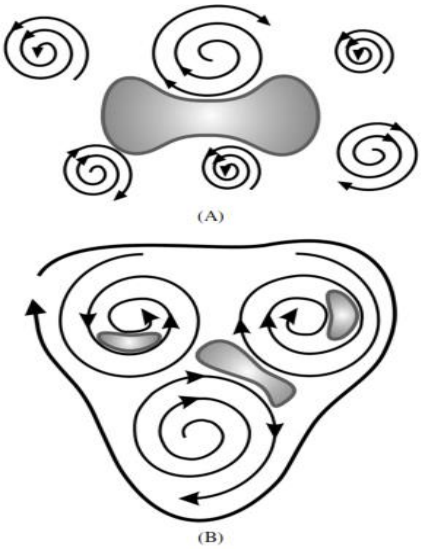

Figure 3. Schematic presentation of the two administrations of emulsification in turbulent flow. (A) Turbulent inertial regime (B) Turbulent viscous regime [28].

A strong shear with high input of energy have to be applied during the process of the homogenization in order to part the drops of a premixed emulsion from the miniaturised scale to the scale of a nano range, consequently, it can overcome the Laplace pressure level [31]. The Laplace pressure causes the imperviousness to droplet disfigurement and separation. At the point when the droplet thickness losses, the Laplace pressure increases effectively [31]. Laplace pressure is the difference in pressure in between the outside and inside of a curving surface [32]. By calculating the pressure that is lost in the gap and adjusting the gap height, the pressure can be controlled. At the point when going through the active region of emulsification found at the gap outlet, the droplets will form a better emulsion and separated [3]. Droplet size was subjected to the homogenization pressure [33].

This review reveals that in HPH, there are shortcomings in understanding the various relationship. The main objectives of this review are:

- Formulate the relationship between homogenising pressure (100-300 MPa) and temperature.
- It is clear that the effect of pressure on the emulsion droplet size is not understood properly. This article will present some insight of the confusion.

It is not possible to measure the velocity fields as flowing in a HPH is exceptionally great, with openings of 10–100 μm and speed of many m/s. Between the valve and valve seat, as the fluid flow through the restricted gap, just before the gap inlet the speed increases on a very short distance [2, 34]. This investigation will be continued on the relationship of velocity and openings.

2. MATHEMATICAL FORMULATION

In high-pressure systems conditional of the flow that steams under high pressure exposed to intense energy changes. In some cases in small disruption valves, experimental design unable to determine the high shear rates and the mechanical stresses and also reveal other phenomena. [2, 21, 22]. So Computational Fluid Dynamic (CFD) provides an alternative cost effective means to simulate the real flows, therefore, complements experimental and theoretical fluid dynamics [35]. CFD compromises an options strategy for a modestly and quickly getting the fields of flows and the characteristics of turbulence locally in the homogenizer [36].

Kleinig and Middelberg [37] used commercial CFD software to calculate the flow pattern in the inlet chamber of the valve in the homogenizer and flow pressure. In the analysis, the flow in the gap was assumed to be laminar eliminating the need for turbulence modelling [37]. The flow in the outlet region was analysed by the same authors in a later publication were the *k*-*ε* model with high Reynold number was used to describe the turbulent exit region [38]. In 1997, Stevenson and Chen had provided the modelling for stream design in the entire valve geometry utilising CFD with standard *k*-ε turbulent model [39]. Miller, et al. [40] applied 2D model with standard k-ε, RNG k-ε, realizable k–ε for flow in a high-pressure homogenising whole valve using CFD [40]. Floury et al. (2004) also used a CFD code for complete valve geometry with RNG *k*-*ε* turbulence models to simulate the flow pattern of an ultra-high homogenizer [2]. Other than that, CFD model was used by Kelly and Muske [41] to measure the hydrodynamic forces through the entire valve in the homogenizer. It is assumed through 2D valve model that in the upstream and within the channel that it has laminar flow, and at the downstream it has turbulent flow. For the downstream feasible k–ε turbulence model has been used [41].

The standard k-ε model was used by Steiner, et al. [27] with low Reynold figure to analyze the 3D in- house valve [27]. Raikar, et al. [42] applied CFD to investigate the homogenizer flow regimes in order to better understand relevant drop breakage mechanisms with standard k-ε turbulent model [42].

Casoli, et al. [43] and Håkansson, et al. [13] also used the standard k-ε model to investigated the homogenising performance of high-pressure homogenizer through the whole valve using CFD [43].

This review considers the computational model of the flow of fluid and offers then an approach to insights into flow regime.

3. COMPUTATIONAL MODELING

By understanding mass plus laws of force conservation, i.e. the Navier–Stokes equation an immediate flow speed and pressure can be gotten. It is expected to have a one stage nonstop flow, incompressible, and isothermal with Newtonian viscosity. [44]. Stevenson and Chen (1997) utilized the model made by Launder & Spalding (1974) that is the standard type of the turbulence model (*k*-*ε* turbulence) (Eqn. (1), (2) and (3)):

$$Continuity \frac{\partial \rho}{\partial t} + \nabla .\left(\rho U \right) = 0 \tag{1}$$

and

$$Momentum \frac{\partial(\rho U)}{\partial t} + \nabla.(\rho U \otimes U) - \nabla.(\mu_{eff} \nabla U = -\nabla p' + \nabla.\left(\mu_{eff}\left(\nabla U\right)^{\mathrm{T}}\right) \quad (2)$$

The *k*--*ε* model for turbulent flow takes on:

$$\mu_{eff} = \mu + \mu_{\mathrm{T}} \text{ where } \mu_{\mathrm{T}} = C_{\mu}\rho\frac{K^2}{\varepsilon} \quad (3)$$

Floury, et al. [45] had used The Stansted high-pressure homogenizer as an operating machine with a steady rate of flow (10 l=h) and little homogenizing valve outline. In the upstream of the valve, it was thought to be absolutely laminar for the stream administration. At the end of the circular channel, the Reynolds number of the downstream which is shaped up by the valve seat is given by

$$Re = \frac{2\rho Q}{\mu\pi r_i} \quad (4)$$

In such spherical pipe geometry, Reynolds number equivalent to about 2000 happen at a move from the laminar raging regime. At operating pressure above 170 x 10^6 Pa, this critical Reynolds number is achieved. At the way out of the valve gap, the flow regime is then interim [2].

For a laminar flow (Eqn. (5) and(6)) which is acquired from Nakayama (1964):

$$\Delta P_L = \frac{\rho}{4}\left[\frac{Q}{2\pi r_e h}\right]^2 + \frac{6\pi Q}{\pi h^3}\mathrm{In}\left(\frac{r_e}{r_i}\right) + \frac{\rho}{2}\left[\frac{Q}{2\pi r_i h}\right]^2 \quad (5)$$

For a system which is transitional (1000 <Re<5000) and acquired from Phipps (1975):

$$\Delta p = \frac{\rho}{4}\left[\frac{Q}{2\pi r_e h}\right]^2 + \frac{5\rho v^{3/5}}{h^3}\left[\frac{Q}{2\pi}\right]^{7/5} \times \left(\frac{1}{r_i^{2/5}} - \frac{1}{r_e^{2/5}}\right) + \frac{\rho}{2}\left[\frac{Q}{2\pi r_i h}\right]^2 \quad (6)$$

As an element of the homogenizing pressure (P_h), the expectations of the extent of the valve gap (h) are conceivable by knowing in the valve, the flow rate (Q), measurements of the seat (r_i, r_e) and characteristics of the liquid for example density ρ, kinematic viscosity ν and viscosity μ

In laminar elongational flow, the deformation time of a droplet is [11]:

$$t_{def} = \frac{\eta_d}{\eta_{elong}.G_{elong}}$$

$$G_{elong} = \frac{\Delta_{P_{elong}}}{\eta_{elong}} \quad (7)$$

As $d_{43} \ \alpha \ P_h^{-0.6}$ (where P_h is the homogenizing pressure), the average droplet size was found to differ [29].

At the channel wall, the shear stress occurred and from restructuring of the Hagen–Poiseuille equation, it can be determined [41]:

$$\tau_{\mathrm{W}} = \frac{\Delta P_e h}{4L} \tag{8}$$

As flow is very extreme, measuring the velocity fields is not possible. Innings et al. (2007) had built up a HPH models which completed from acrylic plastic and made the estimations conceivable. [34]. To scale up a model, Innings et al. (2007) have picked up 2D numbers which are important for the separation procedure; N_{Re}, the Reynolds number, and $N_{\mathrm{G.Kol}}$, the height of turbulent gap (the connection between gap height and Kolmogorov length scale).

The Reynolds number of the gap is defined as (equation 9, 10 and 11):

$$N_{Re} = \frac{h.U_0}{v} \tag{9}$$

And the gap height of the turbulence is defined as

$$N_{G.Kol} = \frac{\text{Gap height}}{\text{Kolmogorov scale}} = \frac{h}{\eta} \tag{10}$$

In a high-pressure homogenizer, for the Kolmogorov scales predictions, the turbulence scales will need to be measured, and the energy dissipation rate will need to be estimated as well.

$$I_0 = \eta.N^{\frac{3}{4}}{}_{Re} = \left(\frac{\frac{v^3}{U^3}}{80h}\right)^{\frac{1}{4}} \cdot \left(\frac{h.U_0}{v}\right)^{\frac{3}{4}} \approx 3h \tag{11}$$

They have demonstrated that it is imaginable to scale-up the field of flow in the hole area if the numbers of Reynolds and the height of turbulent gap are preserved steady [34].

As the fluid velocity and temperature increased, cavitation also increased. Using a dimensionless cavitation number, this can be formalized (Eqn.):

$$\sigma = \frac{P_\infty - P_v(T)}{0.5v^2{}_\infty \rho_L} \tag{12}$$

Where P_∞ is the reference position pressure, Pv(T) the vapor pressure of the fluid at temperature T, v_∞ the speed at the position of the reference and ρ_L the density of the fluid. If the cavitation number is underneath a nascent quality, σ_{inc}, and increments in quality with lower values, cavitation can occur [13].

Operating pressure base of fluid simulation for the space of the gap as an element of working pressure and viscosity (Eqn. (13)) [41]:

$$h = (252 + 2.5\mu)P^{\left(-0.433 + 1.71\times10^{-2}\mu - 1.27\times10^{-3}\mu^2\right)} \tag{13}$$

For the pressure gradient at the inlet of the channel, Kleinig and Middleburg (1996) proposed the following relationship (Eqn. (14)):

$$\Delta P_I = \rho Q^2 \beta^{-1} h^{-3} \tag{14}$$

The loss of pressure over the entire regulator comprises of three sections, an entry loss, an exit loss and a frictional loss.(Eqn. (15)) [39].

$$\frac{2\Delta P}{\rho \bar{u}_i^{\,2}} = K_i + K_t + K_c \tag{15}$$

4. RESULTS AND DISCUSSION:

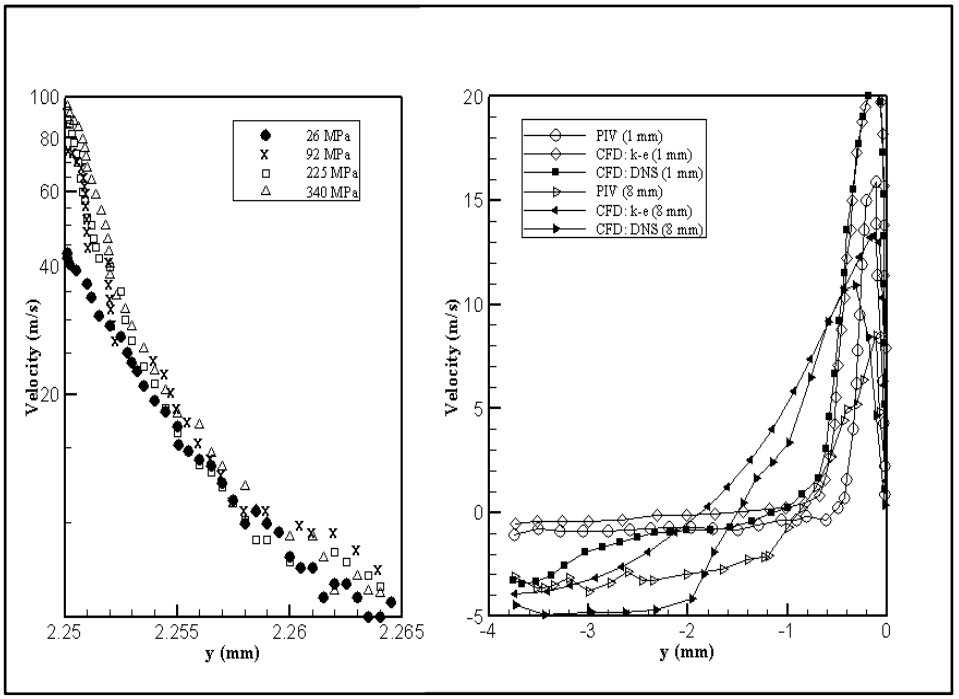

Figure 4. Upstream velocity of the fluid at the slender gap in the middle of the valve and valve seat as a component of working force (26 - 340 MPa) [2] and the examination of the numerical and test longitudinal speed profiles assessed along the channel profundity at two distinct areas behind the processing element: 1 mm and 8 mm [46].

Figure 4 shows the numerical simulations prepared at four dissimilar homogenising pressures (from 26 to 340 MPa) with the RNG k–ε model showed that the intensity of the turbulence flow is very short all everywhere throughout the domain of interest. The data shown for the operating pressure was looked like plotted in one place, but actually, the value of y (mm) was so small that is in between 2.250 to 2.265 mm (Figure 4). However, for the original data [2], figure is not shown, it shows that in between 2.250 to 2.254 mm, there are different in velocity for different operating pressures, with 26 MPa has the lowest velocity (~45 m/s) at 2.250 mm and 340 MPa

has the highest velocity (~100 m/s) at 2.250 mm. After the value of y (mm) is greater than 2.254 mm, the velocity for each operating pressure was decreased continuously. According to the author [2], just before the gap inlet the velocity rapidly increasing up to 100 m/s at a short distance at the highest homogenising pressure when the fluid flows in the regions of restricted flow sections.

For the PIV (Figure 4), the experimental data was obtained from micro-PIV, while for the CFD: k-e and CFD: DNS, the data was obtained from k-e turbulent and direct numerical model, respectively. For the profile situated at 1 mm behind the processing components, it shows the velocity for the numerical and experimental data was highest in between -1 mm and 0 mm, and the results for both numerical and experimental data are about the same, or not so much significant change can be observed. This result was also the same for the profile placed at 8 mm behind the processing foundations except that there were significant changes can be observed in the trial and numerical results. The diminishing resolution of the PIV evaluation in 8 mm is probably due to the existence of the strong opposite flow behind the gap which thus diminishes crest size of the deliberate velocity vectors.

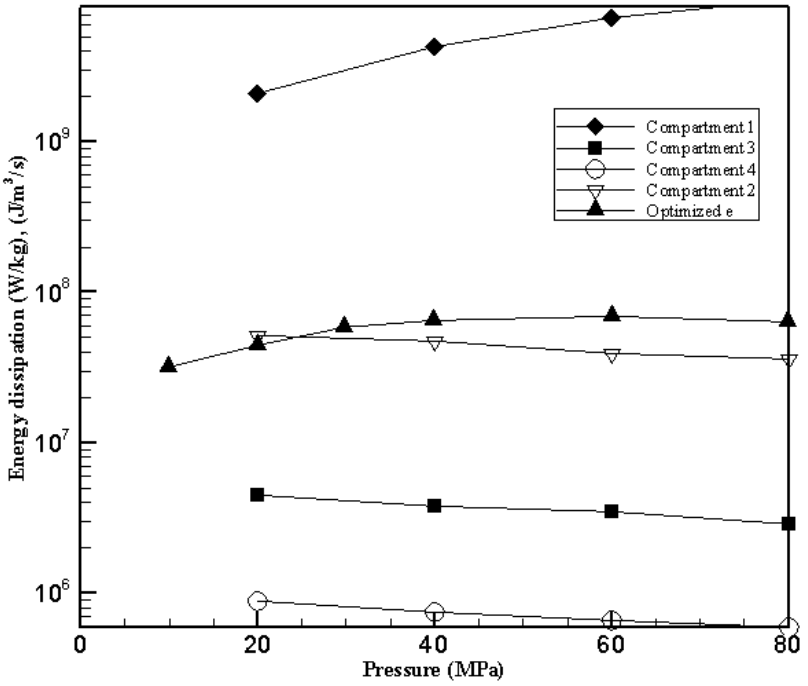

Figure 5. Effects of the normal energy dissipation rate as an element of the droplet of the pressure [47], [48].

An increased in the mean energy dissipation with expanding drop of the pressure in the compartment can be seen. However, the average energy dissemination was somewhat diminishing as compared with other slots. The normal energy dissipation per slot was discovered to be reduced steadily with the gap distance and most astounding specifically after the gap. The first compartment contains the most noteworthy spread in the dissipation of energy. In Table 2, the outcomes getting from the CFD-simulation for each slot are shown. For the optimised energy (e), the energy dissipation rate increased from 10 up to 60 MPa, and after that, the rate decreased.

For the optimized energy dissipation, according to the author [48], it can be accurately fit with a power law equation and a quadratic equation, respectively and thus can allow the model to generate a droplet size distribution data prediction more accurately.

Table 2. Average ($\bar{\varepsilon}$) and maximum ($\varepsilon_{\max}$) turbulent energy dissipation for the compartment [47].

Compartment	$\bar{\varepsilon}$ / W kg^{-1}	$\varepsilon_{\max}$ / W kg^{-1}
1	2.6E + 10	3.3E + 11
2	4.4E + 07	2.9E + 08
3	3.2E + 06	1.1E + 07
4	6.6E + 05	1.6E + 06

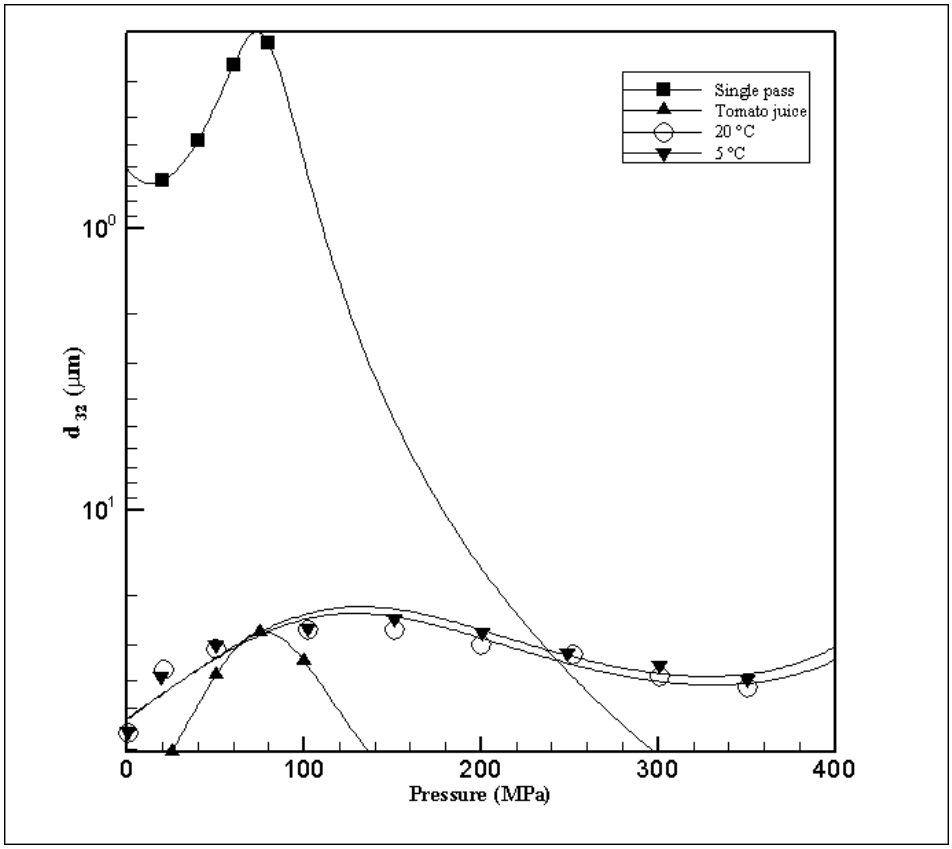

Figure 6. Effect of HPH on a single pass from the four-compartment models, tomato juice mean Sauter diameter and the evolution of mean droplet diameter for methylcellulose emulsions of the early premix temperature [47, 49, 50].

For the particle sizes for the four compartment model at a single pass, it shows that at 20 and 40 MPa, the droplet sizes is larger about 0.7 μm and 0.5 μm , respectively (Figure 6). While as

the pressure increased, the droplet sizes decreased. It was stated by the author, Dubbelboer, et al. [47], that the model underestimated for the pressure at 20 and 40 MPa and overestimated for the pressure at 60 and 80 MPa. While for the emulsion contain tomato juice, it shows that as the pressure increased, the droplet sizes also reduced except that at a pressure of 100 MPa, the droplet sizes is slightly higher than the previous one. For the emulsion which contain methylcellulose, it shows that at the point when the pressure reached up to 150 MPa, both the diameters of the droplets for premix temperature (5 or 20 °C) reduced, however, as the pressure increased more than 150 MPa, the increase of the droplet sizes can be observed. In all cases except the single pass from the four-compartment models, even by using a different procedure, the sizes of the droplet will not be able to reduce below 0.5 μm.

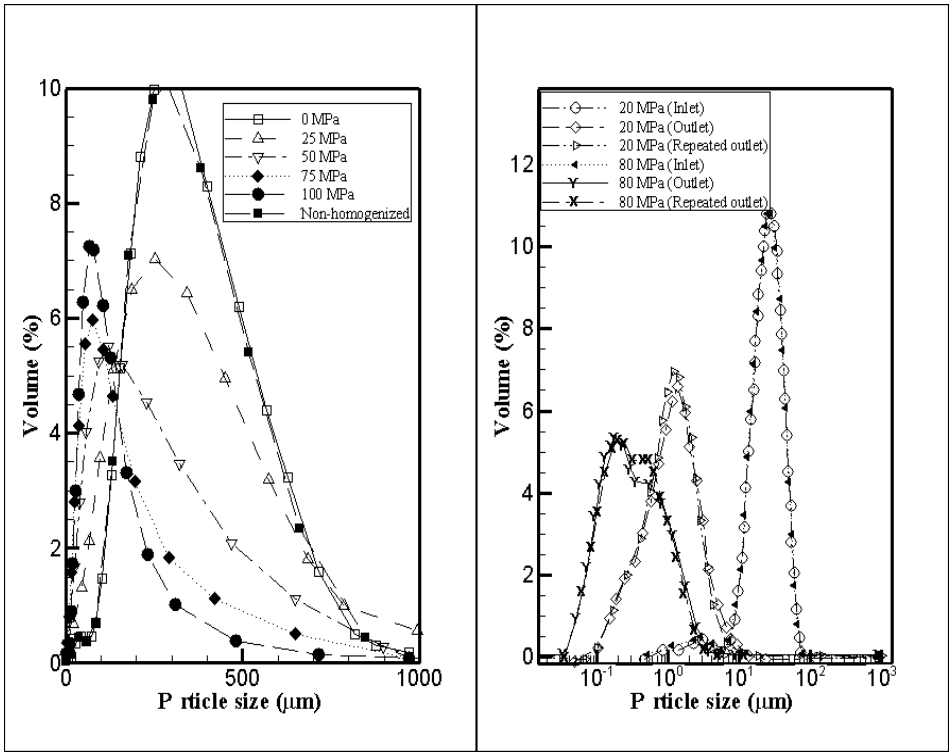

Figure 7. The drop size distribution for the effect of HPH on the tomato juice (0-100 MPa and Non-homogenized) and the homogenization experiment conducted at 20 and 80 MPa at the inlet, outlet, and repeated outlet [47, 49].

For the tomato juice emulsion homogenized at 75 and 100 MPa, it shows a uniform distribution compared to the emulsion homogenized at 0 to 75 MPa (Figure 7). The average particle diameter of the tomato was reduced through the homogenization procedure. On the interruption of suspended particles, through the homogenization treatment at high pressure, it seems to cause smaller changes in the distribution of particle sizes. For the homogenization experiment conducted at the inlet at 20 and 80 MPa shows no changes in the particle size distribution. But there is some changes occur at the outlet where the volume of the particle size distribution reduced at 80 MPa compared to 20 MPa.

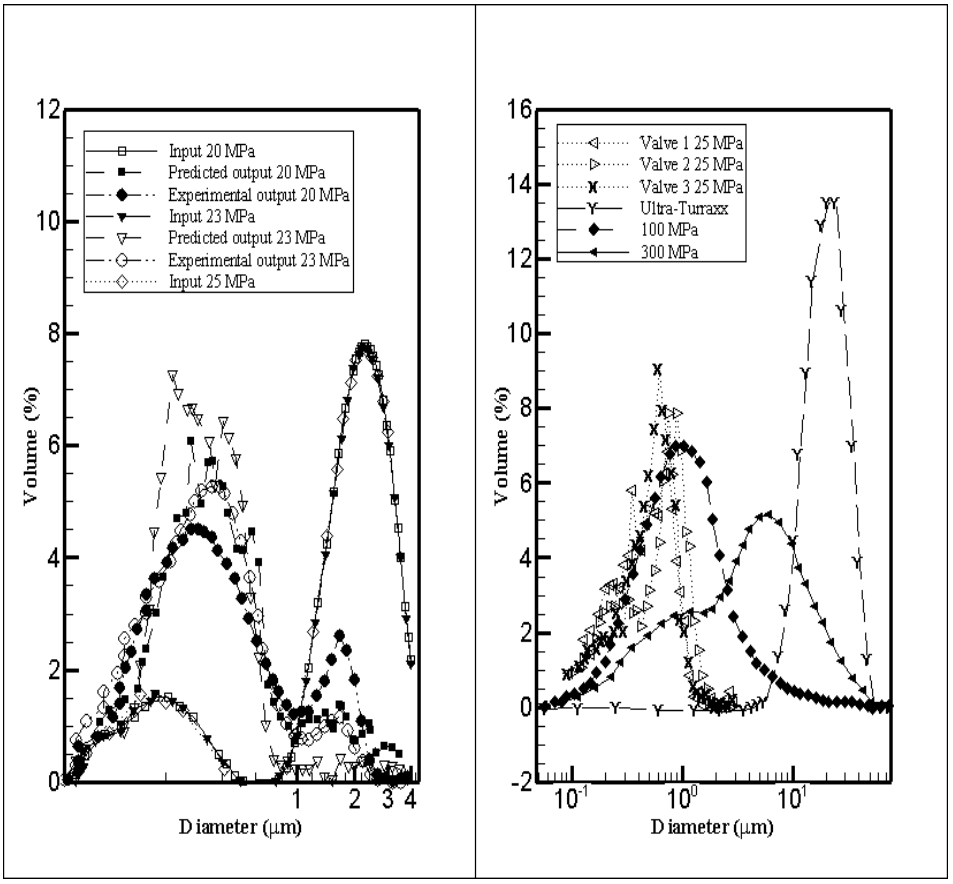

Figure 8. Effects of the droplet diameter distribution at various pressures of the valve performance. The droplet distribution of methylcellulose emulsion in function of the homogenizing process also shown [43, 50].

Figure 8 shows the comparison of the droplet distribution of the experimental data with input and output data. The predicted output curves for the different pressure applied shows results which are almost the same to the trial data. In Figure 8, the comparison for valve performance on the droplet size distribution also shown. For each valve, the homogenizing pressure used is 25 MPa. In contrast, valve 2 is less capable than the other, but the best performance goes to valve 1. Other than that, Ultra-Turrax (Figure 8) has the highest volume percentage, but the droplet sizes are larger, while at 300 MPa, the volume of droplet size distribution is reduced and the droplet sizes also reduced. Based on this results, it suggests that high-pressure treatment can help to reduce the droplet sizes.

Table 3. The experimental studies from various authors on the result of homogenization pressure on the average size of the droplet (d_{32}), the average diameter of the volume (d_{43}), highest diameter (d_{max}) and hydrodynamic diameter (d_H) of O/W emulsions stabilized with a separate type of emulsifier [19].

Author	Emulsifier concentration	Process condition	Droplet size (μm)
Santana, et al. [51]	Collagen fibre (0.5 %)	20-100 MPa (1-2 passes)	1.00-4.05 (d_{32})
de Castro Santana, et al. [52]	Heat treated collagen fibre (0.5 %)	20-100 MPa (1-2 passes)	0.74-3.17 (d_{32})
Schulz and Daniels [33]	Hydroxypropyl methylcellulose (2.5-6 %)	10-160 MPa (1-5 passes)	0.60-6.00 (d_{32})
[53]	Methylcellulose (0.1-2 %)	20-350 MPa (1 pass)	0.40-6.35 (d_{32})
Qian and McClements [54]	ß-lactoglobulin (2 %)	40-1400 MPa (1-8 passes)	0.23-0.15 (d_H)
Perrechil and Cunha [55]	SC (1 %)	10-60 MPa (1 pass)	0.41-1.35 (d_{32})
Seekkuarachchi, et al. [56]	Sodium dodecyl sulphate (1 %)	50-250 MPa (1-20 passes)	0.02-1.00 (d_{32})
Perrechil and Cunha [55]	Tween 20 (1 %)	200-350 MPa (1 pass)	0.12-0.15 (d_{max})
Floury, et al. [29]	WPC (1.5 %)	20-300 MPa (1 pass)	0.25-2.40 (d_{32})
Biasutti, et al. [57]	WPC (1.5 %) and SC (2 %)	15-147 MPa (3 passes)	0.20-0.38 (d_{32})
Desrumaux and Marcand [58]	WPC (1.5 %)	20-350 MPa (1 pass)	0.30-0.70 (d_{32})
Kuhn and Cunha [59]	WPI (3 %)	20-80 MPa (1-7 passes)	0.46-2.17 (d_{43})
Cortés-Muñoz, et al. [31]	WPI (4.3 %)	100-300 MPa (1-3 passes)	0.15-0.45 (d_{43})

Table 3 shows the effects of pressure on the size of emulsions droplet stabilized by biopolymers and surfactants. As can be seen from Table 3, the droplet sizes can be reduced or increased depending on the pressure used and emulsion composition. In the homogenizer, if the recirculation passing numbers increased, a decreased in the emulsion droplet size also can happen. Increasing the amount of time of the emulsion or emulsifier in the valve can enhance adsorption onto the surface of the drops before a collision occurs. The mean diameter of the emulsion can diminish with the pressure of the homogenizer as can be related with the power law equation ($d_{32} \alpha P^{-m}$) [19],[60]. The symbol 'm' in the equation is related to the discontinuity component or Reynolds number, which relies on upon the measurements of the valve, viscosity of the fluid and pressure [19].

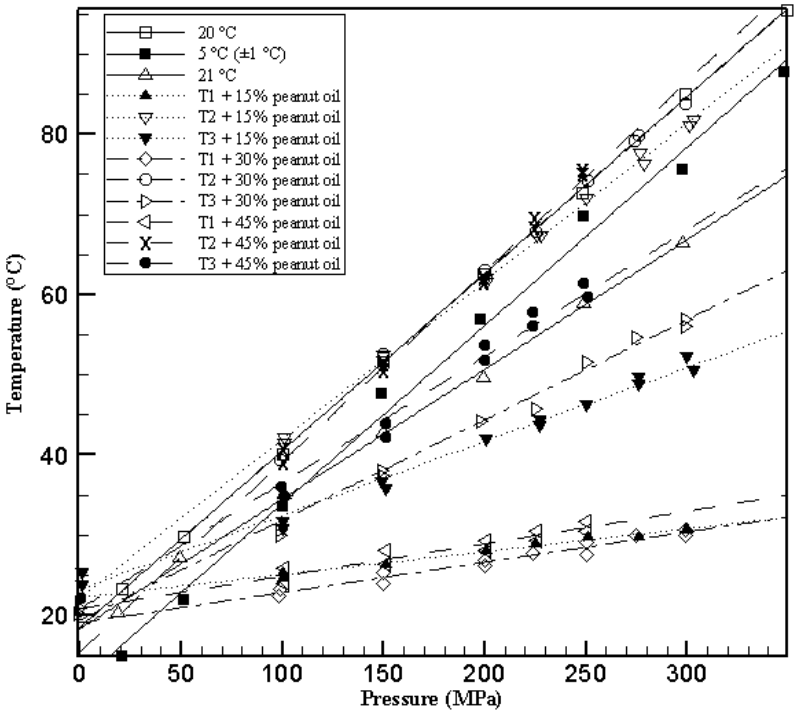

Figure 9. The impacts of pressure from homogenization versus the temperature of the O/W emulsions [50] and O/W emulsions at the exit of the valve [29]. Effect of homogenizing pressure (100-300 MPa) on the temperature measured before the HP-valve (T1), at the HP-valve outlet (T2) and after immediate cooling downstream of the HP-valve (T3) also plotted in the graph [31].

The data in Figure 9 was plotted based on the linear fit curve which can be expressed using Eq.(16), with A and B-coefficients shown in Table 4.

$$\text{Temperature}(°C) = A + B \text{ x Pressure(MPa)} \tag{16}$$

In Figure 9, the outcome of pressure from homogenization on temperature at the valve outlet or the valve end for emulsions which contains 20 wt.% / 0.75 wt.% O/W emulsions shows a rising in temperature as the homogenizing pressure increased for the two temperatures of premix used, 5 and 20 °C, respectively [50]. The liquid flow in the valve has a very high velocity which is what causing the viscous stress and make the fluid warming up. As the temperature ΔT (°C) rising in a streaming fluid of density ρ (kg/m^3) and with a specific heat C_p (J/kg/°C) is corresponding to the homogenizing pressure P (Pa), it can be described as Eq. (16) [50]:

Table 4. A and B –coefficients for the linear equation in Figure 9.

	A-coefficient	B-coefficient
20 °C	18.47	0.22
5 °C (± 1 °C)	11.71	0.22
21 °C	18.31	0.16
T1 + 15% peanut oil	22.22	0.03
T2 + 15% peanut oil	22.25	0.20
T3 + 15% peanut oil	23.24	0.09
T1 + 30% peanut oil	19.06	0.04
T2 + 30% peanut oil	18.47	0.22
T3 + 30% peanut oil	19.39	0.12
T1 + 45% peanut oil	20.84	0.04
T2 + 45% peanut oil	15.44	0.24
T3 + 45% peanut oil	20.77	0.16

$$\Delta T = P/C_p\rho \tag{16}$$

That is why there is a temperature increased for O/W emulsion up to 80 – 90 °C as the pressure is up to about 300 and 350 MPa at the valve exit.

The temperature for the pre-emulsion is 21 °C for O/W emulsion which contains 10 wt.% [29]. From Figure 9, it shows that the temperature at the exit of the homogenizing valve raised from 20.5 to 66.5 °C at 20 and 300 MPa, respectively, with the water-cooling chamber at 5 °C. For this emulsion, when the pressure is utilized until 300 MPa, the temperature did not increase up to 80 or 90 °C like the previous study. This probably due to the characteristics of the emulsion and the cooling water chamber of 5 °C which did not increase the temperature higher.

In Figure 9, the temperature of model emulsions at different stages of the homogenizer during HPH which recorded at different oil concentration of 15, 30 and 45 % also plotted [31]. When no homogenization pressure was applied, the fluid temperature of T1 was close to 22.3 ± 1.9 °C as calculated at the passageway of the HP-valve because of heat exchanges in the middle of the fluid and the intensifier (which are cooling at 10 °C). At different oil concentration (15, 30 or 45%, w/w), the temperatures of the liquid for T1, T2 and T3 raised with the pressure (Figure 9). Temperature which are recorded before the HP-valve (T1) raised by 2.0 ± 0.6 °C, 3.2 ± 0.2 °C or 3.7 ± 0.3 °C per 100 MPa for the respective peanut oil contents (15, 30 or 45%, w/w). This is probably because of the liquid which is compressed in the intensifier during pressure forming up. For T2 which calculated at the HP-valve outlet, at three different oil concentrations (15, 30 or 45%, w/w), it shows increased in temperature by 20.0 ± 0.8 °C, 21.9 ± 0.7 °C or 22.8 ± 0.9 °C per 100 MPa. This increasing in temperature is probably due to the fluid passing through the valve gap and get warmed up and this process mostly related to the kinetic energy transformation into heat. This can be described by $\Delta T_{2\text{-}1}(=T_2\text{-}T_1)$. Depending on the emulsion oil content, different proportions of the input energy could be split into mechanical work and dissipated heat in the HP-valve. While for T3 which is measured after the fluid gets cooled down at the HP-valve outlet shows an increase with temperature by 8.5 ± 0.9 °C, 11.7 ± 0.6 °C or 15.0 ± 1.1 °C per 100 MPa for three different oil concentration respectively. Based on this study and observations from

Figure 9 for T1, T2, and T3, it suggested that the increase in temperatures in the fluid throughout the homogenization treatment does not depend only on the homogenization pressure itself, but the composition of the O/W emulsion also play an important role.

5. CONCLUSION

In high-pressure systems, several factors occur simultaneously such as cavitation, shear stress, and turbulence. The mixture passing through the gap is exposed to shear flow and turbulence, and the pressure transforms into kinetic energy. This leads to the breakup of the droplets into smaller ones. Several studies have been performed before. The results can briefly be listed as below:-

1. The high operating pressure at the way out of the valve causes rising in temperature which can affect the fluid viscosity.
2. Since the velocity can increases (up to 100 m/s) before it reached the gap inlet, it is impossible to calculate the velocity unless the turbulent gap height and the Reynolds number are kept constant.
3. The viscosity of fluid and temperature can be increased due to cavitation.
4. A transition from laminar-turbulent can occur when the pressure is above 170 MPa and a Reynolds number equivalent to around 2000 in the circular duct geometry.
5. With the improvements of the homogenizers design, any pressure losses in the valve can be controlled.

The influence of using high-pressure homogenizer also can affect the distribution of the droplet size, and this depends on the pressure, recirculation numbers and the presence of an emulsifier.

Symbols

k Turbulence kinetic energy (m^2/s^2)

μ Dynamic viscosity (Pa s)

μ_{eff} Effective viscosity (Pa s)

μ_T Turbulent viscosity (Pa s)

$\overline{U_i}$ Velocity at valve gap inlet (m/s)

K_e Exit loss coefficient

K_f Friction loss coefficient

K_i Entrance loss coefficient

Q Flow rate, (kg/m^3)

Re Reynolds number

r_i, r_e Inlet and outlet diameter of the valve seat (m)

TI Turbulent inertial

TV Turbulent viscous

h Valve gap (m)

P_h Homogenising pressure (Pa)

U_o Average gap velocity (m/s)

$N_{G.Kol}$ Relation between gap height and Kolmogorov length scale

I_o Largest eddy (m)

P_∞ Static pressure at a reference position (Pa)

P_v Vapor pressure of water (Pa)

V_∞ Velocity at a reference position (m/s)

η_d Viscosity of continuous phase (Pa s)

η_{elong} Elongational viscosity (Pa s)

$tdiff$ Diffusion time (s)

ΔP_{elong} pressure loss in elongational flow (Pa)

ΔP_i Channel inlet pressure gradient (Pa/m)

ΔP_c Pressure drop across the channel (Pa)

L Channel length (m)

τw Fully developed channel wall shear stress (Pa)

G_{elong} Elongation rate (1/s)

$\otimes$ Tensor Product $(A \otimes B)_{ij}=A_iB_j$

$\nabla.$ Divergence operator

∇ Gradient operator

Greek letters

ε Turbulence energy dissipation (m^2/s^3)

ν Kinematic viscosity (m^2/s)

ρ Density (kg/m^3)

ρ_L Density of liquid water, (kg/m^3)

η Kolmogorov length scale (m)

σ Cavitation number

σ_{inc} Nascent quality

β Proportionality constant

REFERENCES / KAYNAKLAR

[1] J.-W. Kim, D. Lee, H. C. Shum, and D. A. Weitz, "Colloid Surfactants for Emulsion Stabilization," *Advanced Materials*, vol. 20, pp. 3239-3243, 2008.

[2] J. Floury, J. Bellettre, J. Legrand, and A. Desrumaux, "Analysis of a new type of high pressure homogeniser. A study of the flow pattern," *Chemical Engineering Science*, vol. 59, pp. 843-853, 2// 2004.

[3] A. Håkansson, C. Trägårdh, and B. Bergenståhl, "Dynamic simulation of emulsion formation in a high pressure homogenizer," *Chemical Engineering Science,* vol. 64, pp. 2915-2925, 6/15/ 2009.

[4] S.-H. Lee, T. Lefèvre, M. Subirade, and P. Paquin, "Effects of ultra-high pressure homogenization on the properties and structure of interfacial protein layer in whey protein-stabilized emulsion," *Food Chemistry,* vol. 113, pp. 191-195, 3/1/ 2009.

[5] S. Tcholakova, N. D. Denkov, I. B. Ivanov, and B. Campbell, "Coalescence stability of emulsions containing globular milk proteins," *Advances in Colloid and Interface Science,* vol. 123–126, pp. 259-293, 11/16/ 2006.

[6] N. B. Raikar, S. R. Bhatia, M. F. Malone, D. J. McClements, C. Almeida-Rivera, P. Bongers, *et al.*, "Prediction of emulsion drop size distributions with population balance equation models of multiple drop breakage," *Colloids and Surfaces A: Physicochemical and Engineering Aspects,* vol. 361, pp. 96-108, 5/20/ 2010.

[7] S. N. Maindarkar, N. B. Raikar, P. Bongers, and M. A. Henson, "Incorporating emulsion drop coalescence into population balance equation models of high pressure homogenization," *Colloids and Surfaces A: Physicochemical and Engineering Aspects,* vol. 396, pp. 63-73, 2/20/ 2012.

[8] A. Clarke, T. Prescott, A. Khan, and A. G. Olabi, "Causes of breakage and disruption in a homogeniser," *Applied Energy,* vol. 87, pp. 3680-3690, 12// 2010.

[9] J. Floury, A. Desrumaux, M. A. V. Axelos, and J. Legrand, "Degradation of methylcellulose during ultra-high pressure homogenisation," *Food Hydrocolloids,* vol. 16, pp. 47-53, 1// 2002.

[10] Z. Chen, J. Prüss, and H.-J. Warnecke, "A population balance model for disperse systems: Drop size distribution in emulsion," *Chemical Engineering Science,* vol. 53, pp. 1059-1066, 2/6/ 1998.

[11] S. Brösel and H. Schubert, "Investigations on the role of surfactants in mechanical emulsification using a high-pressure homogenizer with an orifice valve," *Chemical Engineering and Processing: Process Intensification,* vol. 38, pp. 533-540, 9// 1999.

[12] F. Innings, L. Fuchs, and C. Trägårdh, "Theoretical and experimental analyses of drop deformation and break-up in a scale model of a high-pressure homogenizer," *Journal of Food Engineering,* vol. 103, pp. 21-28, 3// 2011.

[13] A. Håkansson, L. Fuchs, F. Innings, J. Revstedt, B. Bergenståhl, and C. Trägårdh, "Visual observations and acoustic measurements of cavitation in an experimental model of a high-pressure homogenizer," *Journal of Food Engineering,* vol. 100, pp. 504-513, 10// 2010.

[14] T. Tadros, P. Izquierdo, J. Esquena, and C. Solans, "Formation and stability of nano-emulsions," *Advances in Colloid and Interface Science,* vol. 108–109, pp. 303-318, 5/20/ 2004.

[15] F. A. Perrechil and R. L. Cunha, "Oil-in-water emulsions stabilized by sodium caseinate: Influence of pH, high-pressure homogenization and locust bean gum addition," *Journal of Food Engineering,* vol. 97, pp. 441-448, 4// 2010.

[16] M. B. Essam Hebishy, Buenaventura Guamis, Antonio-José Trujillo, "Stability of Sub-Micron Oil-in-Water Emulsions Produced by Ultra High Pressure Homogenization and Sodium Caseinate as Emulsifier," *Chemical Engineering transactions,* vol. 32, pp. 1813-1818, 2013.

[17] A. Håkansson, L. Fuchs, F. Innings, J. Revstedt, C. Trägårdh, and B. Bergenståhl, "Velocity Measurements of Turbulent Two-Phase Flow in a High-Pressure Homogenizer Model," *Chemical Engineering Communications,* vol. 200, pp. 93-114, 2013/01/01 2012.

[18] G. Narsimhan and P. Goel, "Drop Coalescence during Emulsion Formation in a High-Pressure Homogenizer for Tetradecane-in-Water Emulsion Stabilized by Sodium

Dodecyl Sulfate," *Journal of Colloid and Interface Science,* vol. 238, pp. 420-432, 6/15/ 2001.

[19] R. C. Santana, F. A. Perrechil, and R. L. Cunha, "High- and Low-Energy Emulsifications for Food Applications: A Focus on Process Parameters," *Food Engineering Reviews,* vol. 5, pp. 107-122, 2013/06/01 2013.

[20] S. M. Jafari, E. Assadpoor, Y. He, and B. Bhandari, "Re-coalescence of emulsion droplets during high-energy emulsification," *Food Hydrocolloids,* vol. 22, pp. 1191-1202, 10// 2008.

[21] X. Wu Xue Wu, S. Zhang Shaoying Zhang, and B. Liu Bin Liu, "Study on the Dynamic Pressure Modeling of High-Pressure Jet Homogenization," vol. 1, pp. 284-289, 06/05 2010.

[22] A. Håkansson, F. Innings, C. Trägårdh, and B. Bergenståhl, "A high-pressure homogenization emulsification model—Improved emulsifier transport and hydrodynamic coupling," *Chemical Engineering Science,* vol. 91, pp. 44-53, 3/22/ 2013.

[23] A. Håkansson, L. Fuchs, F. Innings, J. Revstedt, C. Trägårdh, and B. Bergenståhl, "High resolution experimental measurement of turbulent flow field in a high pressure homogenizer model and its implications on turbulent drop fragmentation," *Chemical Engineering Science,* vol. 66, pp. 1790-1801, 4/15/ 2011.

[24] A. Håkansson, L. Fuchs, F. Innings, J. Revstedt, C. Trägårdh, and B. Bergenståhl, "On flow-fields in a high pressure homogenizer and its implication on drop fragmentation," *Procedia Food Science,* vol. 1, pp. 1353-1358, // 2011.

[25] P. Marie, J. M. Perrier-Cornet, and P. Gervais, "Influence of major parameters in emulsification mechanisms using a high-pressure jet," *Journal of Food Engineering,* vol. 53, pp. 43-51, 6// 2002.

[26] J. M. Perrier-Cornet, P. Marie, and P. Gervais, "Comparison of emulsification efficiency of protein-stabilized oil-in-water emulsions using jet, high pressure and colloid mill homogenization," *Journal of Food Engineering,* vol. 66, pp. 211-217, 1// 2005.

[27] H. Steiner, R. Teppner, G. Brenn, N. Vankova, S. Tcholakova, and N. Denkov, "Numerical simulation and experimental study of emulsification in a narrow-gap homogenizer," *Chemical Engineering Science,* vol. 61, pp. 5841-5855, 9// 2006.

[28] N. Vankova, S. Tcholakova, N. D. Denkov, I. B. Ivanov, V. D. Vulchev, and T. Danner, "Emulsification in turbulent flow: 1. Mean and maximum drop diameters in inertial and viscous regimes," *Journal of Colloid and Interface Science,* vol. 312, pp. 363-380, 8/15/ 2007.

[29] J. Floury, A. Desrumaux, and J. Lardières, "Effect of high-pressure homogenization on droplet size distributions and rheological properties of model oil-in-water emulsions," *Innovative Food Science & Emerging Technologies,* vol. 1, pp. 127-134, 6/1/ 2000.

[30] S. M. a. G. Narsimhan, "Coalescence of Protein-Stabilized Emulsions in a High-Pressure Homogenizer," *Journal of Colloid and Interface Science,* vol. 192, pp. 1-15, 1997.

[31] M. Cortés-Muñoz, D. Chevalier-Lucia, and E. Dumay, "Characteristics of submicron emulsions prepared by ultra-high pressure homogenisation: Effect of chilled or frozen storage," *Food hydrocolloids,* vol. 23, pp. 640-654, 2009.

[32] H.-J. Butt, K. Graf, and M. Kappl, *Physics and chemistry of interfaces*: John Wiley & Sons, 2006.

[33] M. B. Schulz and R. Daniels, "Hydroxypropylmethylcellulose (HPMC) as emulsifier for submicron emulsions: influence of molecular weight and substitution type on the droplet size after high-pressure homogenization," *European Journal of Pharmaceutics and Biopharmaceutics,* vol. 49, pp. 231-236, 2000.

[34] F. Innings and C. Trägårdh, "Analysis of the flow field in a high-pressure homogenizer," *Experimental Thermal and Fluid Science,* vol. 32, pp. 345-354, 11// 2007.

[35] C. J. Fletcher, "Computational Fluid Dynamics: An Introduction," in *Computational Techniques for Fluid Dynamics 1*, ed: Springer Berlin Heidelberg, 1998, pp. 1-16.

[36] A. Håkansson, F. Innings, J. Revstedt, C. Trägårdh, and B. Bergenståhl, "Estimation of turbulent fragmenting forces in a high-pressure homogenizer from computational fluid dynamics," *Chemical Engineering Science,* vol. 75, pp. 309-317, 6/18/ 2012.

[37] A. R. Kleinig and A. P. J. Middelberg, "The correlation of cell disruption with homogenizer valve pressure gradient determined by computational fluid dynamics," *Chemical Engineering Science,* vol. 51, pp. 5103-5110, 12// 1996.

[38] A. R. Kleinig and A. P. J. Middelberg, "On the mechanism of microbial cell disruption in high-pressure homogenisation," *Chemical Engineering Science,* vol. 53, pp. 891-898, 2/6/ 1998.

[39] M. J. Stevenson and X. D. Chen, "Visualization of the flow patterns in a high-pressure homogenizing valve using a CFD package," *Journal of Food Engineering,* vol. 33, pp. 151-165, 7// 1997.

[40] J. Miller, M. Rogowski, and W. Kelly, "Using a CFD Model To Understand the Fluid Dynamics Promoting E. coli Breakage in a High-Pressure Homogenizer," *Biotechnology Progress,* vol. 18, pp. 1060-1067, 2002.

[41] W. Kelly and K. Muske, "Optimal operation of high-pressure homogenization for intracellular product recovery," *Bioprocess and Biosystems Engineering,* vol. 27, pp. 25-37, 2004/12/01 2004.

[42] N. B. Raikar, S. R. Bhatia, M. F. Malone, and M. A. Henson, "Experimental studies and population balance equation models for breakage prediction of emulsion drop size distributions," *Chemical Engineering Science,* vol. 64, pp. 2433-2447, 5/15/ 2009.

[43] P. Casoli, A. Vacca, and G. L. Berta, "A numerical procedure for predicting the performance of high pressure homogenizing valves," *Simulation Modelling Practice and Theory,* vol. 18, pp. 125-138, 2// 2010.

[44] A. Håkansson, L. Fuchs, F. Innings, J. Revstedt, C. Trägårdh, and B. Bergenståhl, "Experimental validation of k–ε RANS-CFD on a high-pressure homogenizer valve," *Chemical Engineering Science,* vol. 71, pp. 264-273, 3/26/ 2012.

[45] J. Floury, J. Legrand, and A. Desrumaux, "Analysis of a new type of high pressure homogeniser. Part B. study of droplet break-up and recoalescence phenomena," *Chemical Engineering Science,* vol. 59, pp. 1285-1294, 3// 2004.

[46] S. Blonski, P. M. Korczyk, and T. A. Kowalewski, "Analysis of turbulence in a micro-channel emulsifier," *International Journal of Thermal Sciences,* vol. 46, pp. 1126-1141, 2007.

[47] A. Dubbelboer, J. Janssen, H. Hoogland, A. Mudaliar, S. Maindarkar, E. Zondervan, *et al.*, "Population balances combined with Computational Fluid Dynamics: A modeling approach for dispersive mixing in a high pressure homogenizer," *Chemical Engineering Science,* vol. 117, pp. 376-388, 2014.

[48] S. N. Maindarkar, H. Hoogland, and M. A. Henson, "Achieving Target Emulsion Drop Size Distributions Using Population Balance Equation Models of High-Pressure Homogenization," *Industrial & Engineering Chemistry Research,* vol. 54, pp. 10301-10310, 2015.

[49] M. T. K. Kubo, P. E. Augusto, and M. Cristianini, "Effect of high pressure homogenization (HPH) on the physical stability of tomato juice," *Food research international,* vol. 51, pp. 170-179, 2013.

[50] J. Floury, A. Desrumaux, M. A. V. Axelos, and J. Legrand, "Effect of high pressure homogenisation on methylcellulose as food emulsifier," *Journal of Food Engineering,* vol. 58, pp. 227-238, 7// 2003.

[51] R. Santana, F. Perrechil, A. Sato, and R. Cunha, "Emulsifying properties of collagen fibers: Effect of pH, protein concentration and homogenization pressure," *Food Hydrocolloids*, vol. 25, pp. 604-612, 2011.

[52] R. de Castro Santana, A. C. K. Sato, and R. L. Da Cunha, "Emulsions stabilized by heat-treated collagen fibers," *Food hydrocolloids*, vol. 26, pp. 73-81, 2012.

[53] J. Floury, A. Desrumaux, M. A. Axelos, and J. Legrand, "Effect of high pressure homogenisation on methylcellulose as food emulsifier," *Journal of food engineering*, vol. 58, pp. 227-238, 2003.

[54] C. Qian and D. J. McClements, "Formation of nanoemulsions stabilized by model food-grade emulsifiers using high-pressure homogenization: factors affecting particle size," *Food Hydrocolloids*, vol. 25, pp. 1000-1008, 2011.

[55] F. Perrechil and R. Cunha, "Oil-in-water emulsions stabilized by sodium caseinate: Influence of pH, high-pressure homogenization and locust bean gum addition," *Journal of Food Engineering*, vol. 97, pp. 441-448, 2010.

[56] I. N. Seekkuarachchi, K. Tanaka, and H. Kumazawa, "Formation and charaterization of submicrometer oil-in-water (O/W) emulsions, using high-energy emulsification," *Industrial & engineering chemistry research*, vol. 45, pp. 372-390, 2006.

[57] M. Biasutti, E. Venir, G. Marchesini, and N. Innocente, "Rheological properties of model dairy emulsions as affected by high pressure homogenization," *Innovative Food Science & Emerging Technologies*, vol. 11, pp. 580-586, 2010.

[58] A. Desrumaux and J. Marcand, "Formation of sunflower oil emulsions stabilized by whey proteins with high pressure homogenization (up to 350 MPa): effect of pressure on emulsion characteristics," *International journal of food science & technology*, vol. 37, pp. 263-269, 2002.

[59] K. Kuhn and R. Cunha, "Flaxseed oil–whey protein isolate emulsions: effect of high pressure homogenization," *Journal of Food Engineering*, vol. 111, pp. 449-457, 2012.

[60] L. Phipps, "The fragmentation of oil drops in emulsions by a high-pressure homogenizer," *Journal of Physics D: Applied Physics*, vol. 8, p. 448, 1975.